Accurate Closed-Form Expressions for the Bit Rate-Wireless Transmission Distance Relationship in IR-UWBoF Systems

Mohamed Shehata, *Member, IEEE*, Hassan Mostafa, *Senior Member, IEEE*, and Yehea Ismail, *Fellow, IEEE*

***Abstract*— Efficient utilization of the extremely limited available power of impulse radio ultrawideband (IR-UWB) waveforms can significantly extend their wireless reach in the wireless transmission chain of IR-UWB over fiber (IR-UWBoF) systems. In this letter, the two most common types of photonically generated IR-UWB waveforms are considered and accurate closed-form analytical expressions for the bit rate—distance relationship in the wireless transmission chain of IR-UWBoF systems are developed. These analytical expressions are verified by simulations and optimized such that the wireless transmission distance of IR-UWB waveforms is maximized under the Federal Communications Commission spectral constraints.**

***Index Terms*— Free space path loss (FSPL), impulse radio (IR), microwave photonic (MWP), ultra wideband over fiber (UWBoF).**

I. Introduction

THE severe spectral limits imposed by the FCC on the effective isotropic radiated power (EIRP) of UWB signals [1] is the major factor that tends to limit the maximum wireless propagation distance of these signals. In addition, the wireless transmission of UWB signals is susceptible to the frequency dependent UWB channel loss which further decreases the received signal power. This might prevent a remote wireless user equipment (UE) to access the high speed wireless services offered by UWB systems. A feasable solution to this problem is to employ microwave photonic (MWP) techniques to generate these waveforms in the optical domain and distributing the photonically generated waveforms over optical fiber links to the geographically remote wireless access points at their locations, where IR-UWB signals should be ultimately photodetected and distributed to the UEs over UWB wireless channels. Several approaches have been proposed to demonstrate this efficient integration of hybrid radio frequency (RF) and optical technologies, resulting in the development of IR-UWB over fiber (IR-UWBoF) systems. However, these approaches have been more concerned with the optical generation and transmission processes. This partial, or even complete, ignorance of the wireless transmission part of the IR-UWBoF systems lead to a limited wireless transmission distances that are impractical for high speed services access in realistic scenarios. In [5], a 500 Mbps stream of photonically generated IR-UWB waveforms has been photodetected and transmitted over a UWB wireless channel between two UWB antennas, separated by 65 cm distance apart. In [6], a wireless transmission rate of 1.25 Gbps has been achieved over a distance of about 30 cm. In [7], a higher wireless transmission rate of a 1.625 Gbps has been achieved over a distance of 20 cm. Moreover, a 1.6875 Gbps wireless transmission rate has been used for UWB signalling over 5 cm of wireless transmission [8]. Furthermore, in [9], a bit rate of 3.125 Gbps has been achieved under back-to-back (B2B) wireless transmission. This same rate has been achieved over a wireless transmission distance of 2.9 m [10] by violating the FCC spectral constraints and transmitting the generated waveform using a power spectral density (PSD) limit of -31.3 dBm, which is higher than the admissible FCC PSD by 10 dBm. Only few of the reported techniques have been concerned with the original goal of extending the local wireless reach of high bit rate IR-UWB signals to the practical limits [2]–[4]. Although the aforementioned experimental results confirm the inverse relationship between the transmission bit rate and the transmission distance over a wireless UWB link, the lack of deep theoretical analysis in the reported techniques does not guarantee that the UWB wireless transmission chain is efficiently utilized in terms of the maximum achievable wireless transmission distance and signalling bit rate.

In this letter, the theoretical bit rate - wireless transmission distance relationship is established in terms of the PSD of the transmitted IR-UWB waveforms, considering two common types of the photonically generated IR-UWB waveforms are considered. The rest of this letter is organized as follows. A typical IR-UWBoF transceiver chain is overviewed in Section II, considering the spectra of the two most common types of IR-UWB signals. In Section III, accurate closed form bit rate - distance relationships are developed and analytically evaluated in terms of the IR-UWB signal spectra and the channel model introduced in Section II. The obtained expressions are then numerically evaluated and optimized in Section IV. The obtained results lead to a conclusion which is finally presented in Section V.

II. System Model Overview

Fig.1 shows a simplified transceiver chain of a typical IR-UWBoF system. As shown in this figure, it consists of

Manuscript received June 14, 2017; accepted July 8, 2017. Date of publication July 17, 2017; date of current version October 7, 2017. This work was supported in part by Cairo University, the Zewail City of Science and Technology, in part by AUC, in part by the STDF, in part by Intel, in part by Mentor Graphics, in part by ITIDA, in part by SRC, in part by ASRT, in part by NTRA, and in part by MCIT. The associate editor coordinating the review of this paper and approving it for publication was X. Chu. *(Corresponding author: Mohamed Shehata.)*

M. Shehata is with the Electronics and Communications Engineering Department, Cairo University, Giza 12613, Egypt (e-mail: m.shehata_ieee@yahoo.com).

H. Mostafa is with the Electronics and Communications Engineering Department, Cairo University, Giza 12613, Egypt, also with the Center for Nanoelectronics and Devices, The American University in Cairo, New Cairo 11835, Egypt, and also with the Zewail City of Science and Technology, Giza 12588, Egypt (e-mail: hmoustafa@aucegypt.edu).

Y. Ismail is with the Center for Nanoelectronics and Devices, The American University in Cairo, New Cairo 11835, Egypt, and also with the Zewail City of Science and Technology, Giza 12588, Egypt (e-mail: y.ismail@aucegypt.edu).

Digital Object Identifier 10.1109/LCOMM.2017.2728014

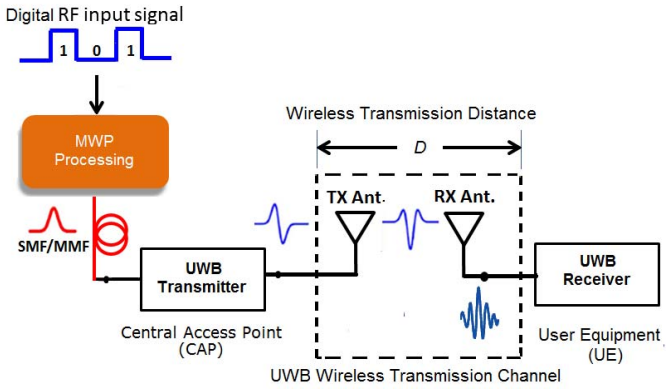

Fig. 1. Block diagram of a typical IR-UWBoF communication system. MWP: microwave photonic, SMF: single mode fiber, MMF: multi mode fiber. Red lines represent optical paths, while black lines represent electrical paths.

a MWP processing stage coupled to an electrical UWB transmitter, which exists in a central access point (CAP), via an optical fiber transmission link, a wireless UWB channel and a UE, where the UWB receiver exists. The input to the MWP processing stage is a sequence of independent and identically distributed (i.i.d) binary data symbols. Within the MWP processing stage, each binary data symbol is encoded by a photonically generated IR-UWB waveform and transmitted over the optical fiber link to the CAP at which the photodetection process is applied. At the CAP, the photodetected waveform is proportional to the m^{th} order derivative of a basis function $\psi\ (t, \tau)$, where τ is its full width at half maximum pulse width. This basis function is an amplitude normalized Gaussian pulse, typically expressed as $\psi\ (t, \tau) = \exp\ (-t^2/{\tau_g}^2)$, or an amplitude normalized sech pulse, expressed as $\psi\ (t, \tau) = sech(t/\tau)$. The FWHM pulse width τ of the input basis function is related to the Gaussian pulse width as $\tau_g \triangleq \tau/2\sqrt{\log\ (2)}$, whereas for the sech pulse is related to τ as $\tau_s \triangleq \tau/2sech^{-1}(0.5)$. In this context, it is assumed that the RF waveform at the TX antenna is related to $\psi\ (t, \tau)$ as $\psi^{(m)}(t, \tau) = \sqrt{E_{b,m}} d^m \psi\ (t, \tau)/dt^m; (t, \tau) \in \mathbf{R}$, where $E_{b,m}$ is the bit energy encoded by the waveform $\psi^{(m)}(t, \tau)$. It is important to note that $E_{b,m}$ is adjusted such that the PSD of the IR-UWB signal does not exceed the maximum PSD admissible by the FCC mask within the useful UWB band between a lower and a higher cutoff frequencies of f_L and f_H, respectively. In particular, $E_{b,m}$ is defined as follows:

$$E_{b,m} \triangleq S_{FCC}(\omega)/\max\left\{\left|\Psi^{(m)}(j\omega, \tau)\right|^2\right\} \quad (1)$$

where $S_{FCC}(\omega)$ is the maximum PSD admissible by the FCC mask within the useful UWB band, $\omega = 2\pi f$ is the angular frequency, $\Psi^{(m)}(j\omega, \tau) = \Im\{d^m \psi\ (t, \tau)/dt^m\}$ and $\Im\{.\}$ denotes the Fourier transform operation. The FCC normalized Fourrier transform of the m^{th} order Gaussian-based derivative is given by

$$\Psi^{(m)}_{n,FCC}(j\omega, \tau_g) = \sqrt{E_{g,m}}(j\omega)^m \tau_g \sqrt{\pi} exp(-(\omega\tau_g)^2/2) \quad (2)$$

where $E_{g,m}$ is the energy of a bit encoded by an m^{th} order Gaussian-based IR-UWB waveform, while the FCC normalized Fourrier transform of the m^{th} order sech-based derivative is given by

$$\Psi^{(m)}_{n,FCC}(j\omega, \tau_s) = \sqrt{E_{s,m}}(j\omega)^m 4\pi\ \tau_s \text{sech}(2\pi\omega\tau_s) \quad (3)$$

where $E_{s,m}$ is the energy of a bit encoded by an m^{th} order sech-based IR-UWB waveform. Throughout the rest of this letter, $\Psi^{(m)}_{n,FCC}(\omega, \tau)$ refers to one of the definitions in (2) or (3) as required. Substituting each of the definitions in $\partial\left|\Psi^{(m)}_{n,FCC}(\omega, \tau)\right|^2/\partial\omega = 0$ and solving for ω yields the peak emission angular frequencies $\omega_{p,g}$ and $\omega_{p,s}$, defined as the angular frequencies at which $\left|\Psi^{(m)}(j\omega, \tau)\right|^2 = \max\left\{\left|\Psi^{(m)}(j\omega, \tau)\right|^2\right\}$ for Gaussian and sech-based IR-UWB waveforms, respectively. The corresponding bit energies $E_{g,m}$ and $E_{s,m}$ are obtained by

$$E_{g,m} = S_{FCC}(\omega) \exp\left((\omega_{p,g}\tau_g)^2/2\right)/\omega^{2m}_{p,g}\pi\tau_g^2 \quad (4)$$

$$E_{s,m} = S_{FCC}(\omega)\cosh^2\left(2\pi\omega_{p,s}\tau_s\right)/\omega^{2m}_{p,s}(4\pi\tau_s)^2 \quad (5)$$

It is assumed that the IR-UWB waveforms are transmitted over a typical path loss channel with an arbitrary path loss exponent γ. In this context, the squared magnitude frequency response of this channel model $PL(\omega)$ is expressed as [11]

$$PL(\omega) = \frac{G_{TX}(\omega)G_{RX}(\omega)c^2}{4\omega^2 D^\gamma} \quad (6)$$

where $G_{TX}(\omega)$ and $G_{RX}(\omega)$ are the frequency responses of the UWB transmit and receive antennas respectively, c is the speed of light and D is the wireless transmission distance between the transmit and receive antennas. The spectral and the spatial characteristics of both antennas depend on the particular design of each antenna. For simplicity, both antennas are assumed to have a piecewise flat frequency response over the useful UWB band and their radiation patterns are aligned in the directions of their maximum radiation. Therefore, $G_{TX}(\omega)$ and $G_{RX}(\omega)$ are replaced by the constants G_{TX} and G_{RX}, respectively.

III. Bit Rate - Distance Relationship

In general, there is an inverse relationship between the transmission bit rate and the wireless transmission distance. According to [12], the exact form of this relationship is expressed in terms of the UWB signal spectrum and the free space path loss (FSPL) channel model as follows:

$$D = \left(\frac{1}{2\pi\left(\frac{E_b}{N_o}\right)R_b k_B T_o.NF.LM}\int_{\omega_L}^{\omega_H} PL(\omega)\Phi(\omega)d\omega\right)^{1/\gamma} \quad (7)$$

where E_b/N_o is the bit energy to noise PSD ratio, R_b is the bit rate of the UWB wireless transmission link, k_B is the Boltzmann constant and *To* is the nominal receiver noise temperature, *NF* is the noise figure, *LM* is the link margin, $\omega_H = 2\pi f_H, \omega_L = 2\pi f_L$ and $\Phi\ (\omega)$ is the PSD of the transmitted IR-UWB waveform, normalized to the maximum admissible FCC PSD. The value of E_b/N_o depends on the

particular modulation scheme and is given by the inverse bit error rate (BER) function of this modulation scheme such that the BER does not exceed the limit value of 10^{-3} without forward error correction (FEC). Substituting (6) in (7), the bit rate - distance relationship can be re-defined as follows:

$$D = \lambda R_b^{-1/\gamma} \tag{8}$$

where

$$\lambda \triangleq \left(\frac{G_{TX} G_{RX} c^2}{8\pi \left(\frac{E_b}{N_o}\right) k_B T_o . NF . LM} \int_{\omega_L}^{\omega_H} \omega^{-2} \Phi(\omega) d\omega \right)^{1/\gamma} \tag{9}$$

Clearly, the proportionality constant λ relates the transmission distance and the bit rate in terms of the wireless UWB link design parameters as well as the parameters of the IR-UWB waveform. The value of λ for Gaussian and sech input basis functions are denoted by $\lambda_{g,m}$ and $\lambda_{s,m}$, respectively. The value of $\lambda_{g,m}$ is obtained by substituting (2) in (9) as follows:

$$\lambda_{g,m} \triangleq \left(\frac{(c\tau_g)^2 G_{TX} G_{RX} E_{g,m}}{8 \left(\frac{E_b}{N_o}\right) k_B T_o . NF . LM} \int_{\omega_L}^{\omega_H} \omega^{\mu} \exp\left(-(\omega\tau_g)^2\right) d\omega \right)^{1/\gamma} \tag{10}$$

where $\mu = 2m - 2$. Similarly, the value of $\lambda_{g,m}$ is obtained by substituting (3) in (9) as follows:

$$\lambda_{s,m} = \left(\frac{2\pi (c\tau_s)^2 G_{TX} G_{RX} E_{s,m}}{\left(\frac{E_b}{N_o}\right) k_B T_o . NF . LM} \int_{\omega_L}^{\omega_H} \omega^{\mu} \mathrm{sech}^2 (2\pi\omega\tau_s) d\omega \right)^{1/\gamma} \tag{11}$$

The analytical solution of (10) is given by

$$\lambda_{g,m} = \beta_g \Big[Q(\omega_H \tau_g/\sqrt{2}) - Q(\omega_L \tau_g/\sqrt{2}) \Big]^{1/\gamma} \tag{12}$$

where

$$\beta_g = \left(\frac{(c\tau_g)^2 G_{TX} G_{RX} E_{g,m}}{16 \left(\frac{E_b}{N_o}\right) k_B T_o . NF . LM} \left(\frac{\sqrt{2}}{\tau_g}\right)^{\mu+1} \right)^{1/\gamma} \tag{13}$$

and

$$Q(u) = (1-q)\Gamma\left(\frac{\mu+q+1}{2}\right) erf(u) - \exp(-u^2) \times \sum_{n=0}^{L-1} \frac{\Gamma\left(\frac{\mu+1}{2}\right)}{\Gamma\left(\frac{\mu+1}{2} - n\right)} u^{\mu-2n-1} \tag{14}$$

where Γ (.) is the gamma function defined as $\Gamma(z) = \int_{y=0}^{\infty} y^{z-1} \exp(-y) dy$ and $erf(z) = (2/\sqrt{\pi}) \int_{-\infty}^{z} \exp(-y^2) dy$ is the Gaussian error function. On the other hand, the analytical solution of (11) for sech-based IR-UWB waveforms is given by

$$\lambda_{s,m} = \beta_s [\Lambda(2\pi\omega_H\tau_s) - \Lambda(2\pi\omega_L\tau_s)]^{1/\gamma} \tag{15}$$

where

$$\beta_s = \left(\frac{2\pi (c\tau_s)^2 G_{TX} G_{RX} E_{s,m}}{\left(\frac{E_b}{N_o}\right) k_B T_o . NF . LM} \left(\frac{1}{2\pi\tau_s}\right)^{\mu+1} \right)^{1/\gamma} \tag{16}$$

and

$$\Lambda(\mathrm{u}) = \sum_{l=0}^{\infty} \sum_{\rho=0}^{\mu} \frac{(-1)^{l+\rho}(l+1)}{(\mu-\rho)!(-2(l+1))^{\rho+1}} u^{\mu-\rho} \times \exp(-2(l+1)u) \tag{17}$$

The design of an efficient IR-UWB wireless transmission link is therefore reduced to the optimization of λ with respect to one or more of the controllable set of these parameters such as the waveform type, its derivative order, the modulation scheme, the targeted BER performance using this scheme and the spectral and spatial characteristics of the TX and/or RX UWB antennas. Throughout the rest of this letter, the optimization of λ is confined to the set of controllable waveform parameters, which are the type of the input basis function, its FWHM pulse width and its derivative order m.

IV. Simulation Results and Analysis

In this section, the bit rate - distance proportionality constant λ in (9) is evaluated for Gaussian and sech-based IR-UWB waveforms according to the analytical expressions in (12) and (15) and verified by applying numerical intergrations to their counterparts in (10) and (11), respectively. The considered value of the path loss exponent $\gamma = 3.5$ is assumed to express typical large scale propagation loss in UWB wireless channels. Derivative orders m are assumed to take values through $\{1, 2, ...7\}$. Based on the FCC spectral regulations in [1], $f_L = 3.1$ GHz, $f_H = 10.6$ GHz and $\max\{S_{FCC}(\omega)\} = -41.3$ dBm/MHz. The values of the Boltzmann constant and the nominal receiver noise temperature are $k_B = 1.23 \times 10^{-38}$ J/K and $T_o = 300$ K, respectively. Throughout the simulations, on off keying (OOK) modulation is assumed. Consequently, the corresponding value of E_b/N_o required to achieve the FEC BER limit of 10^{-3} is 10 dB. The TX and RX UWB antennas are assumed to have identical characteristics such that $G_{TX}(\omega) = G_{RX}(\omega) = 1$. The simulaion starts by evaluating the values of the sets $(\tau_g, \omega_{p,g}, E_{g,m})$ and $(\tau_s, \omega_{p,s}, E_{s,m})$.

Fig.2 depicts the variation of the wireless transmission distance $\lambda_{g,m} R_b^{-\gamma}$ with τ for Gaussian-based IR-UWB waveforms at the considered values of m and $R_b = 2.5$ Gbps. Obviously, there exists an optimum FWHM input pulse width at which the wireless reach of the m^{th} order Gaussian-based IR-UWB waveform attains its maximum value. Non-optimal FWHM input pulse widths limits the wireless reach of the IR-UWB waveform below its maximum value. Moreover, the Gaussian-based monocycle pulse achieves the absolute maximum wireless transmission distance of about 4.18 m at an optimum FWHM pulse width of 69.76 ps. Similarly, Fig.3 presents the variation of $\lambda_{s,m} R_b^{-\gamma}$ with τ for the sech-based IR-UWB waveforms at the same values of m and R_b as in Fig. 2. It is clear that the sech monocycle pulse outperforms its higher order derivatives and achieves a maximum wireless

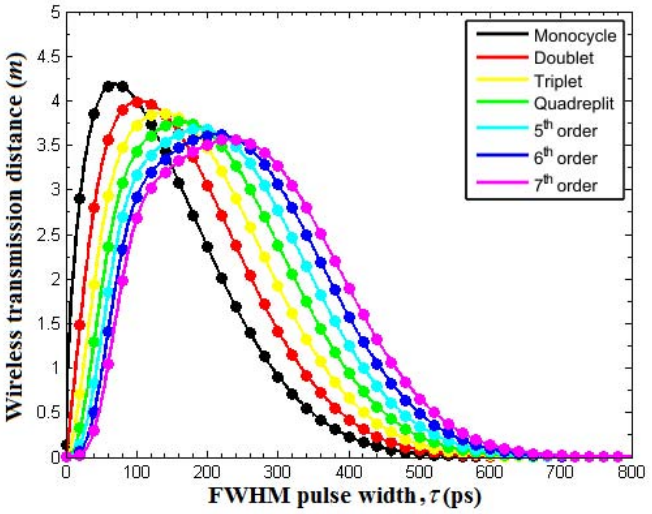

Fig. 2. Wireless transmission distance versus the FWHM pulse width of the Gaussian-based IR-UWB waveforms. Solid lines: theoretically obtained results. Markers: Results obtained by numerical integration techniques.

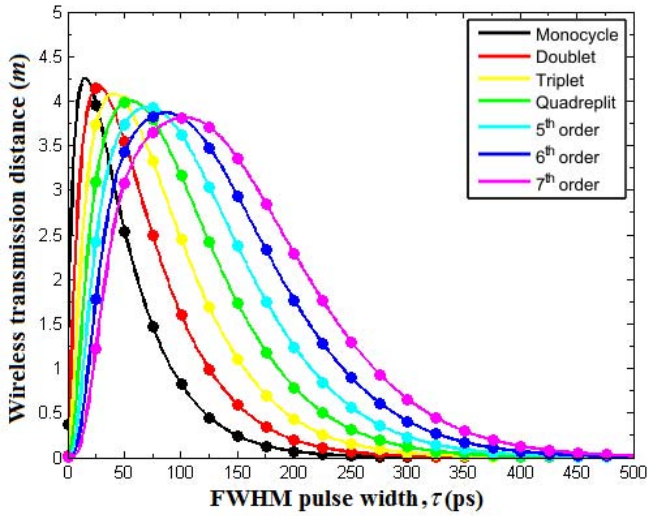

Fig. 3. Wireless transmission distance versus the FWHM pulse width of the sech-based IR-UWB waveforms. Solid lines: theoretically obtained results. Markers: Results obtained by numerical integration techniques.

transmission distance of about 4.26 m at an optimum FWHM pulse width of 15.13 ps. To compare the derivatives of each waveform types, it is more useful to assume that the range of τ consists of three sub-ranges: R_1, R_2 and R_3. For FWHM input pulse widths having $0 \leq \tau \leq 101.8$ ps for Gaussian input basis functions and $0 \leq \tau \leq 22.14$ ps for a sech input basis function, $\lambda_{g,m} > \lambda_{g,n}(\tau)$ and $\lambda_{s,m} > \lambda_{s,n}(\tau)$, for $m < n$. Wihtin the second sub-range, R_2, corresponding to $101.8 < \tau \leq 240.3$ ps for Gaussian input basis functions and $22.14 < \tau \leq 100.3$ ps for sech input basis functions, the wireless transmission distance using an m^{th} order IR-UWB waveform can outreach another n^{th} order waveform of the same type and FWHM pulse width τ, depending on the particular values of m, n and τ, where $\lambda_{g,m}(\tau) \underset{<}{\overset{>}{=}} \lambda_{g,n}(\tau)$ and $\lambda_{s,m}(\tau) \underset{<}{\overset{>}{=}} \lambda_{s,n}(\tau)$ for $m \neq n$. For the third sub-range R_3, corresponding to $240.3 < \tau$ ps for Gaussian input basis functions and $100.3 < \tau$ ps for sech input basis functions, the situation in R_1 is reversed and the wireless reach of an n^{th} order IR-UWB waveform is larger than that of an m^{th} one having the same pulse width, $m < n$. Although the differences in the wireless transmission distances achievable by both waveform types are not quite large, sech-based IR-UWB waveforms still outperform their Gaussian-based counterparts in terms of the small pulse widths at which these distances are achieved. This advantage is always desirable in high bit rate IR-UWBoF systems.

V. Conclusion

In this letter, accurate closed form expressions for the bit rate - distance relationship in wireless IR-UWB systems are derived in terms of the spectra of the wireless transmitted waveforms. It is shown that the wireless transmission distance can be maximized by tuning the pulse widths of these waveforms. Two very common types of IR-UWB waveforms are considered which are based on the derivatives of Gaussian and sech pulses. Simulation results confirm the accuracy of the developed expressions and indicate that excessive differentiation of Gaussian and sech-based IR-UWB waveforms tends to limit the maximum wireless transmission distance that can be achieved using these two waveform types.

References

[1] "First report and order, (revision of part 15 of the commission's rules regarding ultra-wideband transmission systems)," U.S. Federal Commun. Commission, Washington, DC, USA, Tech. Rep. FCC 02-48, Feb. 2002.

[2] R. Rodes *et al.*, "Range extension and channel capacity increase in impulse-radio ultra-wideband communications," *Tsinghua Sci. Technol.*, vol. 15, no. 2, pp. 169–173, Apr. 2010.

[3] J. B. Jensen, R. Rodes, A. Caballero, X. Yu, T. B. Gibbon, and I. T. Monroy, "4 Gbps impulse radio (IR) ultra-wideband (UWB) transmission over 100 meters multi mode fiber with 4 meterswireless transmission," *Opt. Exp.*, vol. 17, no. 19, pp. 16898–16903, Sep. 2009.

[4] R. Rodes, J. B. Jensen, A. Caballero, X. Yu, S. Pivnenko, and I. T. Monro, "Enhanced bit rate-distance product impulse radio ultra-wideband over fiber link," *Microw. Opt. Technol. Lett.*, vol. 52, no. 7, pp. 1679–1680, Jul. 2010.

[5] M. Abtahi, M. Mirshafiei, S. LaRochelle, and L. A. Rusch, "All-optical 500-Mb/s UWB transceiver: An experimental demonstration," *J. Lightw. Technol.*, vol. 26, no. 15, pp. 2795–2802, Aug. 1, 2008.

[6] Y. M. Chang, J. Lee, D. Koh, H. Chung, and J. H. Lee, "Ultrawideband doublet pulse generation based on a semiconductor electroabsorption modulator and its distribution over a fiber/wireless link," *IEEE/OSA J. Opt. Commun. Netw.*, vol. 2, no. 8, pp. 600–608, Aug. 2010.

[7] H. Shams, A. Kaszubowska-Anandarajah, P. Perry, and L. P. Barry, "Optical generation, fiber distribution and air transmission for ultra wide band over fiber system," in *Proc. Opt. Fiber Commun. Conf. Expo. (OFC)*, Mar. 2009, pp. 1–3, paper OWR2.

[8] S. Pan and J. Yao, "Photonic generation of chirp-free UWB signals for UWB over fiber applications," in *Proc. IEEE Int. Topical Meet. Microw. Photon. (MWP)*, Oct. 2009, pp. 1–4.

[9] E. Zhou, X. Xu, K.-S. Lui, and K. K.-Y. Wong, "High-speed photonic power-efficient ultra-wideband transceiver based on multiple PM-IM conversions," *IEEE Trans. Microw. Theory Techn.*, vol. 58, no. 11, pp. 3344–3351, Nov. 2010.

[10] T. B. Gibbon *et al.*, "3.125 Gb/s impulse radio ultra-wideband photonic generation and distribution over a 50 km fiber with wireless transmission," *IEEE Microw. Wireless Compon. Lett.*, vol. 20, no. 2, pp. 127–129, Feb. 2010.

[11] T. Wang, W. Heinzelman, and A. Seyedi, "Link energy minimization in IR-UWB based wireless networks," *IEEE Trans. Wireless Commun.*, vol. 9, no. 9, pp. 2800–2811, Sep. 2010.

[12] M. Ghavami, L. Michal, and R. Kohno, *Ultra Wideband Signals and Systems in Communication Engineering*, 2nd ed. West Sussex, U.K.: Wiley, 2007.